

Min YUN, Yang LIU, Lian-zhong DENG, Qi ZHOU, Jian-ping YIN

Generation of CW cold CH₃CN molecular beam by a bent electrostatic quadrupole guiding: Monte-Carlo study

© Higher Education Press and Springer-Verlag 2008

Abstract A new kind of continuous-wave (CW) cold molecular beam, methyl cyanide (CH₃CN) beam, is generated by a bent electrostatic quadrupole guiding. The Stark shift of rotational energy levels of CH₃CN molecule and its population distribution are calculated, and the dynamic processes of electrostatic guiding and energy filtering of CH₃CN molecules from a gas source with room temperature (300 K) are simulated by Monte Carlo Method. The study showed that the longitudinal and transversal temperatures of output cold CH₃CN beam could be about ~2 K and ~420 mK, and the corresponding guiding efficiency was about 10⁻⁵ as the guiding voltage was 3 kV. Furthermore, the temperature of the guided molecules and its guiding efficiency can be controlled by adjusting the guiding voltages applied on electrodes.

Keywords trapping, Zeeman and Stark effect, atomic and molecular beam sources and techniques, methyl cyanide

PACS numbers 33.80.Ps, 33.55.Be, 39.10.+j

1 Introduction

Cold molecules play the key part in high-resolution spectroscopy [1] and precise measurement [2], studying of cold chemical reaction and cold collisions [3–5], interferometry

of matter wave [6], quantum computing and its information possessing [7–8] and so on. The cooling and trapping of molecules have become one of hot research points in the fields of molecular physics, molecule optics, quantum optics and quantum information science, etc.

Cold, slow molecular beams are of wide utility. A common use of such beam is a source for loading into traps, where the particles can be further cooled and manipulated. Because the number of trapped particles is typically limited by the characteristics (flux, forward velocity, temperature, etc.) of the initial beam, work on producing cold molecular beam sources has recently been an actively research field, such as slowing a molecule beam using rapidly rotator [9], decelerating supersonic polar molecular beams with time-varying electric field [10–12], filtering effusive beam [13, 14] by bent guiding, ejecting cold molecule beam from buffer gas cooled samples [15–17], optical stark decelerating [18], etc. Most molecules, which are going to be cooled, need to be specially pre-produced. For example, some of them are ablated from metal target by pulsed laser (e.g. PbO, CaH), some free radical molecules are produced by pulsed electric discharge (e.g. OH) or photodissociation (e.g. CH), the preparation of the others are expensive (e.g. ND₃, D₂O). However, their dipole moments are not large, so high external fields are needed. Therefore, it is of great significance to produce cold molecular beam coming from easily achieved inorganic or organic molecules with a large dipole moment that can be widely used in cold molecular physics and spectroscopy, even in cold chemistry.

In this paper, we use a bent electrostatic guiding scheme to produce continuous-wave (CW) cold methyl cyanide (CH₃CN) beam, and study the dynamic process of electrostatic guiding and energy filtering of CH₃CN molecules by Monte-Carlo simulations, and obtain some new and inter-

Min YUN, Yang LIU, Lian-zhong DENG, Qi ZHOU, Jian-ping YIN (✉)

State Key Laboratory of Precision Spectroscopy, Department of Physics, East China Normal University, Shanghai 200062, China
E-mail: jpyin@phy.ecnu.edu.cn

Received November 5, 2007; accepted December 2, 2007

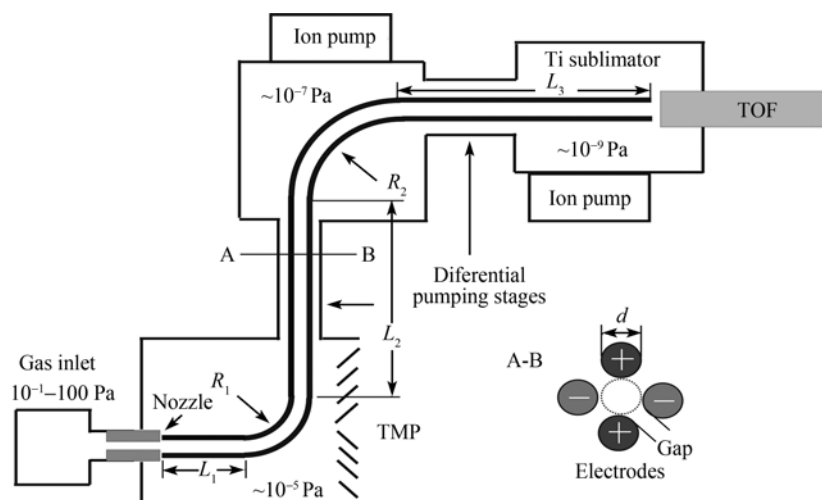


Fig. 1 Scheme of the electric quadrupole guiding. Inset (A-B) is the arrays of the electrodes. The dotted circle at the center of the four electrodes is the guiding region.

esting results. CH_3CN is common reagent and organic solvent in chemistry, and can be widely used in laser chemistry research. Furthermore, it is also an important interstellar probe-molecule for astronomical objects in astrophysics and for research of molecule spectroscopy [19]. CH_3CN has a relative large electric dipole moment of 3.91 Debye, which can be easily controlled with relatively low electrostatic field.

2 Electrostatic bent guiding scheme

Figure 1 shows our scheme to generate a CW cold CH_3CN beam by using a bent quadrupole guiding, which is formed by four S-shaped charged stainless-steel electrodes with a 3-mm diameter, and the corresponding gap between the surfaces of neighboring electrode is 1 mm. The neighboring electrodes carry opposite charges with the same magnitude.

In Fig. 1, the effusive molecular beam (its mean free path is larger than the diameter of the nozzle) is generated from a gas cell with a pressure of 10^{-1} –300 Pa. The curvature radii of the bent electrodes at the first and second bends are $R_1 = 12.5$ mm and $R_2 = 25$ mm, respectively. Most of the molecules will not be guided and escaped from our quadrupole guiding tube due to their kinetic energies (either the longitudinal or transversal) exceed the Stark guiding potential, and molecules with a kinetic energy lower than the Stark potential will be guided and detected with a home-made time of flight (TOF) mass spectrometer. So this bend guiding system, as a low-pass energy filter, can be used to generate a CW cold molecular beam. In order to measure the longitudinal velocity distribution of the guided cold molecular beam with the TOF technique, we use a pulsed high voltage switch to

charge our quadrupole electrodes with the same pulse cycle as one of the YAG laser. We designed a time-sequence control system and use a frequency-quadrupled pulsed light of the Nd: YAG laser (Surelite II-10, 266 nm, 10 Hz and 100 mJ) to ionize the guided cold molecules. The pressures in three vacuum chambers are 10^{-5} Pa, $\sim 10^{-7}$ Pa and $\sim 10^{-8}$ Pa (even $\sim 10^{-9}$ Pa) respectively, which will be obtained by tube molecule pump (TMP), ion pump and Ti sublimator.

We use finite element software to calculate the spatial electrostatic field distribution of our charged-wire layout (four charged electrodes), and the results are shown in Fig. 2. We can see from Fig. 2 that the resulting electric strength is linearly proportional to the voltages U applied on electrodes and the radial position r within a guiding region ($r \leq r_0$, as shown the vertical dotted lines in Fig. 1), and the electro-

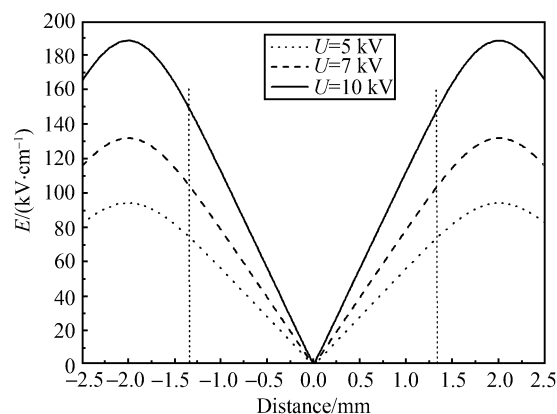


Fig. 2 The radial distribution of the electric field produced by our charged quadrupole electrodes, and the vertical dotted lines represent the maximum effective guiding region ($r \leq r_0$) of cold polar molecules in a hollow electrostatic guiding tube.

static field is a quadrupole field distribution (like a hollow electrostatic tube) with a zero central E-field value, which can be used to guide cold polar molecules in the weak-field-seeking (WFS) states.

3 Theoretical calculation and analysis

3.1 Stark shift of rotation energy levels of methyl cyanide

From Stark effect, the Stark potential for the guided molecules is given by $W_{\text{Stark}} = -\boldsymbol{\mu} \cdot \mathbf{E}$, and the corresponding Stark interaction gradient force is $\mathbf{F} = -\nabla(\boldsymbol{\mu} \cdot \mathbf{E})$, where $\boldsymbol{\mu}$ is the electric dipole moment of the molecule, and \mathbf{E} is the vector of electric field. When $\boldsymbol{\mu}$ is antiparallel to the \mathbf{E} , the molecules in the WFS states will be repelled to the minimum of the field.

CH₃CN is a kind of polyatomic symmetric top molecule, and the rotational constants of its ground state ($v=0$) are $A=158\,099.022\,1$ MHz and $B=9198.899\,141$ MHz, respectively [19]. The rotational energy can be calculated by

$$W_{\text{rot}} = h[BJ(J+1) + (A-B)K^2 - D_J J^2 (J+1)^2 + D_{JK} J(J+1)K^2 + D_K K^4] \quad (1)$$

where J is the rotational quantum number, and K is the projection of J on the molecule's symmetry axis. If the molecule is not considered as rigid, the last three terms (correct terms) in Eq.(1) are necessary, where $D_J=3.807\,445$ kHz, $D_{JK}=0.177\,404\,8$ MHz, and $D_K=2.83$ MHz. A Coriolis interaction between vibration and rotation states splits the levels where $K \neq 0$ into two components. The inversion split-

ting W_{inv} of the vibrational state is the order of 10^{-3} cm⁻¹. The Stark shift of the symmetric top molecule in the electric field can be expressed as

$$W_{\text{Stark}} = \pm (W^{(1)} + W^{(2)}) \quad (2)$$

where

$$W^{(1)} = \mu |\mathbf{E}| \frac{MK}{J(J+1)} \quad (3)$$

and

$$W^{(2)} = \frac{\mu^2 |\mathbf{E}|^2}{2hB} \left\{ \frac{(J^2 - K^2)(J^2 - M^2)}{J^3(2J-1)(2J+1)} - \frac{[(J+1)^2 - K^2][(J+1)^2 - M^2]}{(J+1)^3(2J+1)(2J+3)} \right\} \quad (4)$$

are the first- and second-order Stark effect, respectively. μ denotes the electric dipole moment of the polar molecule, M is the projection of J on the electric field \mathbf{E} , h denotes the Planck constant. The plus and the minus signs of the Stark shift W_{Stark} represent the WFS and Strong-field-seeking (SFS) states, respectively. The total energy is given by $W = W_{\text{rot}} + W_{\text{Stark}}$.

Figure 3 shows the total energy W (including Stark shift) of a CH₃CN molecule in the generated inhomogeneous electrostatic field for $J=1, 2$ and 3. It is clear from Fig. 3 that with the increasing of the electric field E , the nonlinear Stark effects become more remarkable, and the energy levels with an increasing E -field dependence show the WFS states of CH₃CN molecule, which can be guided in a hollow electrostatic tube.

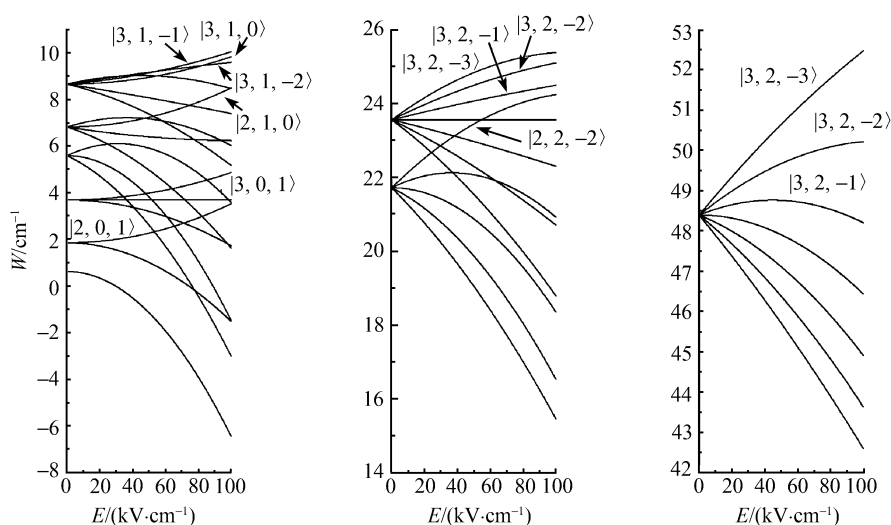


Fig. 3 Total energies W of several rotational states ($J=1, 2$, and 3) of CH₃CN molecule as the function of the electric field E . Some WFS states are shown by labels, the others are the SFS ones.

Figure 4 shows the dependence of the Stark shift W_{Stark} on the rotational energy W_{rot} for all WFS states with a quantum number of $J = 0$ to 50. We can see from Fig.4 that the distribution range of the Stark shift W_{Stark} is very wide, not concentrated on the several special rotational states. Each W_{rot} belongs to a particular $|J, K\rangle$ state, which holds the W_{Stark} with the number of $2J+1$ because of the existing of M quantum number. When J is increased to 50, there are totally 176 850 states and about half of them are WFS states, so the simulation of the molecular motion in all WFS states is impossible for our PC (Personal Computer) system. So it is necessary to simplify the simulation without changing the characters of guiding. In the guide, the changes of molecular velocities and positions mostly depend on W_{Stark} . As the molecules with a larger W_{Stark} will suffer a larger gradient force and are apt to stay in the guide, we classify all the WFS states of the molecules into tens of representative states according to their W_{Stark} (e.g., the states whose W_{Stark} are between 1.0 cm^{-1} and 1.1 cm^{-1} are represented by the state with W_{Stark} as 1.05 cm^{-1} , such as the state $|9, -3, 5\rangle$) [20]. So we can choose about 60 representative states to represent all the WFS states with the W_{Stark} up to 6 cm^{-1} , as shown in Fig.4. The variation range of Stark shift represented by each representative state is $\pm 0.05 \text{ cm}^{-1}$, and the difference of Stark shift between two adjacent representative states is defined as 0.1 cm^{-1} .

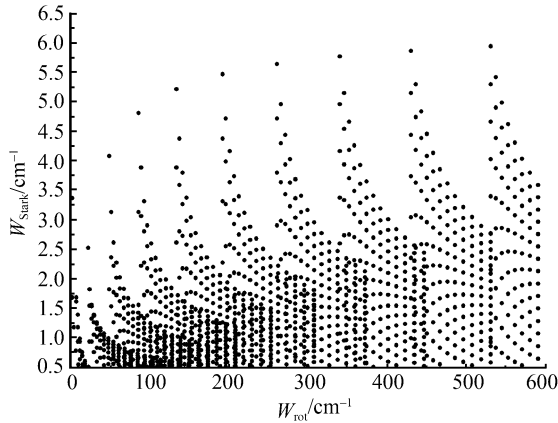


Fig.4 The dependence of the Stark shift of CH_3CN molecule in the 100 kV/cm electric field on the rotational energy for the rotational quantum number of $J=0$ to 50.

3.2 Populations at rotation energy levels of CH_3CN molecule

The population of the rotational energy level of ground-state molecule follows the Boltzmann distribution. For CH_3CN , a kind of symmetric top molecule, the distribution is given by [21]

$$F_{JK} = \frac{F_v g_J g_K g_I}{Q_r} \exp\left(-\frac{E_{J,K}}{k_B T}\right) \quad (5)$$

and

$$Q_r = \frac{1}{\sigma} \sum_{J=0}^{\infty} \sum_{K=-J}^J (2J+1) \exp\left(-\frac{E_{J,K}}{k_B T}\right) \approx \frac{1}{\sigma} \sqrt{\frac{\pi}{B^2 A} \left(\frac{k_B T}{h}\right)^3} \quad (6)$$

where F_v denotes the percent of molecules at the different vibrational energy level. Such as $F_v = 1$ shows that all molecules are at the lowest vibrational energy level. $g_J = 2J+1$, $g_K = 1$ for $k=0$ and $g_K = 2$ for $k \neq 0$. $E_{J,K} = W_{\text{rot}}$ is the rotational energy. T is the rotational temperature (in our case, $T=300 \text{ K}$). k_B is Boltzmann constant. The symmetric degree σ is 3 for methyl cyanide that belongs to C_{3v} symmetric group. The weight of degenerated nuclear spin g_I has different expressions, which depends on K quantum number, that is,

$$g_I = \frac{1}{3} \left[1 + \frac{1}{(2I+1)^2} \right], \quad k = 0, 3, 6, \dots$$

$$g_I = \frac{1}{3} \left[1 - \frac{1}{(2I+1)^2} \right], \quad k \neq 0, 3, 6, \dots \quad (7)$$

where $I = 1/2$ is the spin of the three off-axis atoms H. Figure 5 shows the dependence of the relative population or abundance (triangle dots) at the rotational level on the rotational quantum number J , which presents a classical Boltzmann distribution. Since the rotational temperature of our effusive molecular beam is 300 K , the rotational states with a rotational quantum number of $J=0$ to 50 occupy more than 99% of the population. Among them 51% are the WFS states. The dependence of the relative population on the Stark shifts (see the squared dots in Fig.5) for a given E -field strength of 100 kV/cm tells us the population of each representative states in the simulation. Although the population of CH_3CN molecules with a lower Stark shift is larger, most of them will escape from the electrostatic guiding tube because the interaction gradient force acted on them is weaker. Other molecules in the rotational states with a higher Stark shift will be apt to pass through the bent guiding and to form a cold molecular beam, but their population is less. Thus the guiding efficiency and the translation temperature of the guided cold molecular beam will depend on the contribution of those representative states with different Stark shift. Here we choose 60 representative states in our simulation.

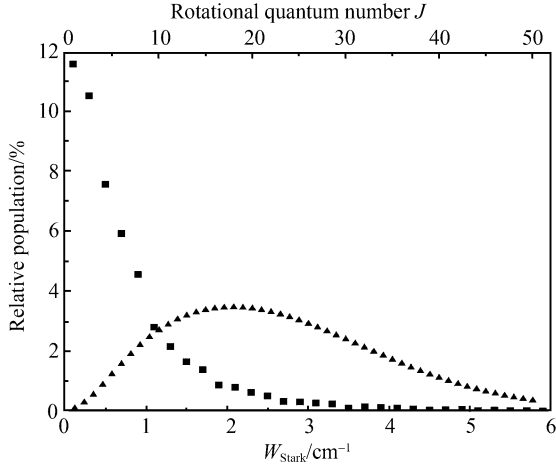


Fig. 5 Relative population (*squared dots*) vs. Stark shift for the field strength of 100 kV/cm at $T=300$ K. The triangle dots show the relative population via the rotational energy level for $J=0-50$.

4 Monte-Carlo simulations and its results

In this subsection we study the dynamic process of guiding CH_3CN molecules by using Monte-Carlo simulations. The molecules originate from an effusive source at room temperature ($T=300$ K) with a small exit channel (nozzle) through which the gas flows from the high pressure side ($10^{-1}-100$ Pa) to the low pressure side (10^{-5} Pa). Directly behind the nozzle, the molecules are injected into our hollow electrostatic quadrupole tube. The transversal velocity distribution of state-selected molecules is the Boltzmann distribution,

$$P(v_\rho) = \frac{1}{\alpha_\rho \sqrt{\pi}} e^{-v_\rho^2/\alpha_\rho^2}, \quad |v_\rho| < |v_{\max}| \quad (8)$$

with $\alpha_\rho = \sqrt{2k_B T_\rho / m}$ is the mean square root velocity, the transverse velocity $v_\rho = \sqrt{v_x^2 + v_y^2}$ and the maximum transverse caught velocity v_{\max} , which depends on the transverse Stark trapping potential for CH_3CN molecules in our electrostatic quadrupole guiding tube. The longitudinal velocity distribution is

$$P(v_z) = \frac{2v_z}{\alpha_z^2} e^{-v_z^2/\alpha_z^2} \quad (9)$$

with $\alpha_z = \sqrt{2k_B T_z / m}$. The initial temperature of molecules injected into the guide is $T_\rho = T_z = 300$ K. Longitudinal velocity filtering is achieved by bending the guiding tube with a suitable radius of curvature. If the molecule is too fast, the centrifugal force of molecular motion at the bend will

exceed its Stark interaction force, it will escape from the guide and lost.

We start the simulation with the conditions of $U=\pm 7$ kV, $L_1=100$ mm, $L_2=360$ mm, $L_3=260$ mm. The maximum electric-field strength in the guiding regime is about 100 kV/cm, and the initial number of the guided molecules in our simulation is 2×10^7 and they are distributed representatively in about 60 representative WFS states according to Fig.5. Since the initial longitudinal most probable velocity of the effusive molecular beam with a translation temperature of 300 K is 280 m/s, the movement of the guided molecules in the hollow electrostatic tube can be regarded as a classical one, and will satisfy a Newton motional equation: $m\ddot{\mathbf{r}} = \mathbf{F}(\mathbf{r}) = -\nabla W_{\text{Stark}}(\mathbf{r})$.

The results of the Monte-Carlo simulations are shown in Figs.6 and 7, which show the longitudinal and transversal velocity distributions of input (before guide) and output (after guide) molecular beams. In Figs.6 (b) and 7(b), the data points with a error bar are our simulated results, and the solid line is the fitted curve from Eqs.(9) and (10), and we obtain $\alpha_z = 55$ m/s, $T_z = 7.5$ K and $\alpha_\rho = 27.4$ m/s, $T_\rho = 1.8$ K. We can see from Figs.6 and 7 that the longitudinal and transverse velocity distributions of output molecular beam are narrower than that of input molecular one, and the most probable velocity of the later is lower than that of the former, because most of the hot molecules with a higher longitudinal and transverse velocity are escaped from the electrostatic guide. The guiding efficiency is $\sim 10^{-4}$, which can be obtained from the ratio of the integrated area under the longitudinal or transverse velocity profiles of the output molecular beam [the dotted line in Fig. 6(a) or 7(a)] to that of the input beam [the solid line in Fig. 6(a) or 7(a)].

Furthermore, we also study the dependences of the longitudinal (and transverse) temperature of the guided molecular beam and the guide efficiency η on the guiding voltage V , and the simulated results are shown in Fig.8. We can find from Fig.8 that with the decreasing of guiding voltages from 8 kV to 3 kV, the longitudinal and transverse temperatures of the guided molecular beam will be decreased linearly from $T_z=9.2$ K and $T_\rho=2.32$ K to $T_z=2.2$ K and $T_\rho=420$ mK, and the corresponding guiding efficiency will be reduced quadratically from 1.51×10^{-4} to 1.96×10^{-5} . That is, the dependences of the temperature T of the guided cold molecular beam and its guide efficiency η on the guiding voltage V are given by $T \propto V$ and $\eta \propto V^2$. This shows that the lower the guiding voltage is, the less the number of guided cold molecules is, and the lower the temperature of the out-

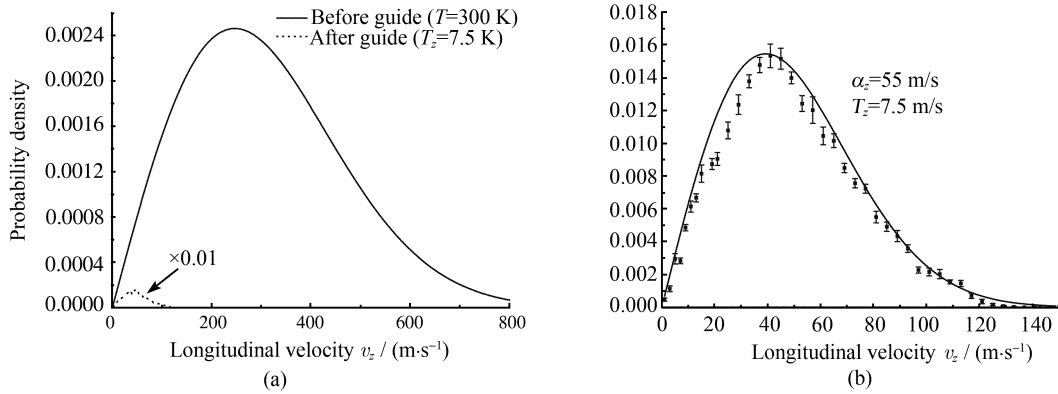


Fig. 6 (a) Longitudinal velocity distributions of molecules before guiding (*solid line*) and after guiding (*dotted line*) for 7 kV guiding voltage; (b) Enlargement of the dotted line in (a) with error bars and fitted curves of longitudinal velocity distribution of output molecular beam.

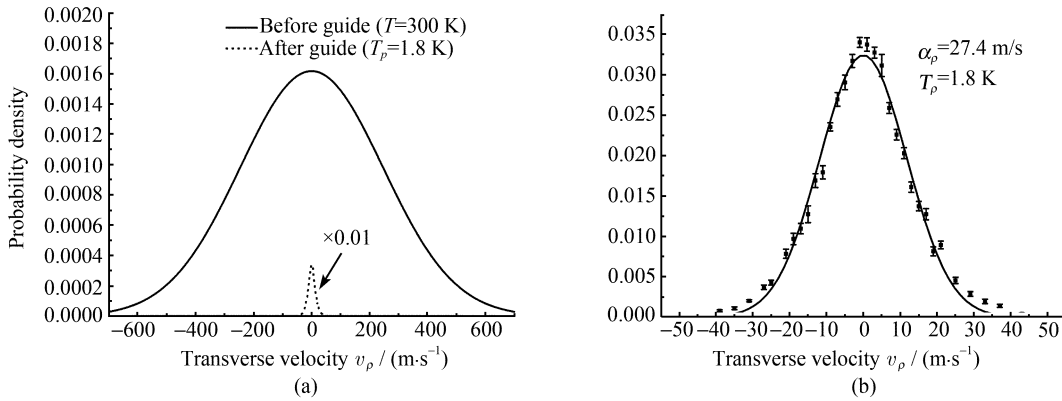


Fig. 7 (a) Transversal velocity distributions of molecules before guiding (*solid line*) and after guiding (*dotted line*) for 7 kV guiding voltage; (b) Enlargement of the dotted line in (a) with error bars and fitted curves of transverse velocity distribution of output molecular beam.

put molecular beam is. Since the typical flux of input effusive molecular beam is about $10^{15}/\text{s}$, we can generate a CW cold molecular beam with a translation temperature of ~ 2 K and a flux of $\sim 10^{10}/\text{s}$ by using our bent quadrupole electrostatic guiding when the guiding voltage is $V=3$ kV.

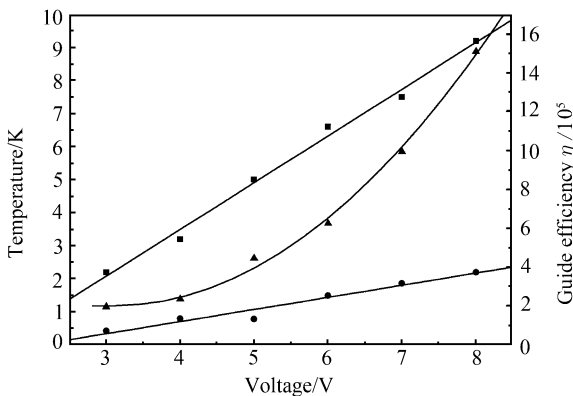


Fig. 8 Dependences of the longitudinal temperature (T_z , *squared dots*), transversal temperature (T_p , *circular dots*) and the guide efficiency (η , *triangle dots*) on the guiding voltages V . Solid lines are fitting curves.

5 Conclusion

In this paper, we have used the bent quadrupole electrostatic field to generate a CW cold methyl-cyanide (CH_3CN) molecular beam, and calculated the Stark energy shift of CH_3CN molecule in our guiding field and the population distribution of rotational energy levels of the CH_3CN molecules. We also study the dynamic process of electrostatic guiding and energy filtering of CH_3CN molecules by using Monte-Carlo simulation. Our study shows that our bent quadrupole electrostatic guiding scheme can be used to produce a CW cold molecular beam, and its longitudinal and transversal temperatures are ~ 2 K and ~ 420 mK, respectively as the temperature of the input effusive beam is 300 K. The corresponding output flux is about $\sim 10^{10}/\text{s}$. In addition, the temperatures of the guided molecular beam and its output flux can be controlled by adjusting the guiding voltages applied on the electrodes. If an effusive molecular beam with a temperature of ~ 8 K pre-cooled by ^4He buffer gas cooling [17] is used, we could obtain a colder molecular beam with a temperature of lower than ~ 30 mK, which can

be loaded into a typical electrostatic or optical trap for further cooling, and also have some important applications in the fields of cold molecular physics and molecule optics, cold molecular spectroscopy and cold chemistry, and so on.

Acknowledgements This work was supported by the National Nature Science Foundation of China under Grant Nos.10374029, 10434060 and 10674047, by the National Key Basic Research and Development Program of China under Grant No. 2006CB921604, and by the Science and Technology Commission of Shanghai Municipality Nos. 2006CB921604 and 07JC14017.

References

1. J. J. Hudson, B. E. Sauer, M. R. Tarbutt, and E. A. Hinds, *Phys. Rev. Lett.*, 2002, 89(2): 023003
2. D. DeMille, F. Bay, S. Bickman, D. Kawall, D. Krause Jr., S. E. Maxwell, and L. R. Hunter, *Phys. Rev. A*, 2000, 61(5): 052507
3. N. Balakrishnan and A. Dalgarno, *Chem. Phys. Lett.*, 2001, 341: 652
4. K. Burnett, P. S. Julienne, P. D. Lett, E. Tiesinga, and C. J. Williams, *Nature*, 2002, 416 : 225
5. E. Bodo, F. A. Gianturco, and A. Dalgarno, *J. Chem. Phys.*, 2002, 116(21): 9222
6. B. Brezger, L. Hackermüller, S. Uttenthaler, J. Petschinka, M. Arndt, and A. Zeilinger, *Phys. Rev. Lett.*, 2002, 88(10): 100404
7. D. DeMille, *Phys. Rev. Lett.*, 2002, 88(6): 067901
8. A. André, D. DeMille, J. M. Doyle, M. D. Lukin, S. E. Maxwell, P. Rabl, R. J. Schoelkopf, and P. Zoller, *Nature Physics*, 2006, 2(9): 636
9. M. Gupa and D. Herschbach, *J. Phys. Chem. A*, 2001, 105(9): 1626
10. H. L. Bethlem, G. Berden, and G. Meijer, *Phys. Rev. Lett.*, 1999, 83(8) : 1558
11. M. R. Tarbutt, H. L. Bethlem, J. J. Hudson, V. L. Ryabov, V. A. Ryzhov, B. E. Sauer, G. Meijer, and E. A. Hinds, *Phys. Rev. Lett.*, 2004, 92(17): 173002
12. J. R. Bochinski, Eric R. Hudson, H. J. Lewandowski, G. Meijer, and Jun Ye, *Phys. Rev. Lett.*, 2003, 91(24): 243001
13. S. A. Rangwala, T. Junglen, T. Rieger, P. W. H. Pinkse, and G. Rempe, *Phys. Rev. A*, 2003, 67(4) : 0434061
14. T. Rieger, T. Junglen, S. A. Rangwala, G. Rempe, and P. W. H. Pinkse, *Phys. Rev. A*, 2006, 73(6): 061402
15. M. S. Elioff, J. J. Valentini, and D. W. Chandler, *Science*, 2003, 302: 1940
16. Dima Egorov, Thierry Lahaye, Wieland Schollkopf, Bretislav Friedrich, and John M. Doyle, *Phys. Rev. A*, 2002, 66(4) : 043401
17. S. E. Maxwell, N. Barhms, R. deCarvalho, D. R. Glenn, J. S. Helton, S. V. Nguyen, D. Patterson, J. Petricka, D. DeMille, and J. M. Doyle, *Phys. Rev. Lett.*, 2005, 95(17) : 173201
18. R. Fulton, A. I. Bishop, and P. F. Baker, *Phys. Rev. Lett.*, 2004, 93(24) : 243004
19. M. Simeckova, S. Urban, U. Fuchs, F. Lewen, G. Winnewisser, I. Morino, and K. M. T. Yamada, *J. Mol. Spectros.*, 2004, 226 : 123
20. T. Junglen, *Guiding and Trapping of Cold Dipolar Molecules*, doctoral thesis, 2005: 17; and private discussion with Pinkse (from Rempe's group, Max-Planck Institute of Germany)
21. W. Gordy and Robert L. Cook, *Microwave Molecular Spectra*, New York: Wiley-Interscience, 1984: 54